DOI: 10.1002/chem.200802209

Acceleration of Reductive Elimination of [Ar-Pd-C_{sp^3}] by a Phosphine/Electron-Deficient Olefin Ligand: A Kinetic Investigation

Heng Zhang,[a] Xiancai Luo,[a] Kittiya Wongkhan,[b] Hui Duan,[a] Qiang Li,[a] Lizheng Zhu,[a] Jian Wang,[c] Andrei S. Batsanov,[b] Judith A. K. Howard,[b] Todd B. Marder,*[b] and Aiwen Lei*[a, d]

Abstract: The kinetics of the reductive elimination step of a C_{sp^3}–C_{sp^2} Negishi cross-coupling catalyzed by a 1:1 complex **2** of palladium and the phosphine/electron-deficient olefin ligand (*E*)-3-(2-diphenylphosphanylphenyl)-1-phenyl-propenone (**1**) was studied. Complex **2** is an exceptionally efficient and highly selective catalyst for Negishi cross-coupling reactions involving primary and secondary alkylzinc reagents bearing β-hydrogen atoms. Turnover numbers (TONs) as high as 10^5 and turnover frequencies (TOFs) as high as $1000\ s^{-1}$ were observed. The reactions occurred rapidly and selectively even at 0 °C. The fact that the reaction was first order in [Pd] is consistent with homogeneous catalysis by Pd complexes rather than by Pd nanoparticles (NPs). Through systematic kinetic investigations of the Negishi coupling of ethyl 2-iodobenzoate with alkylzinc chlorides, the rate constants for reductive elimination of [Ar-Pd-C_{sp^3}] were determined to be $>0.3\ s^{-1}$, which is about 4 or 5 orders of magnitude greater than the values previously reported for [Pd(dppbz)] and [$Pd(PPh_3)_2$] systems (dppbz = 1,2-bis(diphenylphosphino)-benzene). The use of a 2:1 ratio of **1**:Pd resulted in reduced catalytic activity and selectivity, presumably because the olefin moiety could no longer assist in the reductive elimination step. Importantly, hydrogenation of the C=C double bond in ligand **1** generated a saturated ligand (**1**H_2), which was not only less effective than **1**, but also gave rise to substantial amount of ethylbenzoate formed by competing β-hydride elimination. Thus, the π-accepting olefin moiety in **1** must enhance reductive elimination rates, and, consequently, inhibit formation of byproducts resulting from β-hydride elimination.

Keywords: cross-coupling · kinetics · olefins · palladium · reductive elimination

Introduction

Transition-metal-catalyzed cross-coupling reactions are widely used in organic synthesis.[1,2] However, the transformations involving alkyl groups remain problematic due to slow reductive elimination (i.e., C_{sp^2}–$C_{sp^2} > C_{sp^2}$–$C_{sp^3} > C_{sp^3}$–C_{sp^3}) with deleterious but fast β-H elimination.[3–5] Culkin and Hartwig investigated the reductive elimination of complex **A** through stoichimetric reactions (Scheme 1), and found the half life of the complex at 40 °C to be 23 min, corresponding to a rate constant of about $5\times10^{-4}\ s^{-1}$ (Scheme 1).[6] Espinet et al. reported the rate constant for reductive elimination of complex **B** to be $8.9\times10^{-6}\ s^{-1}$ at 25 °C (Scheme 1).[7] Some progress has been made to promote the rate of oxidative addition by employing sterically hindered and/or electron-rich ligands.[4,8–17] Although the steric hindrance assists the reductive elimination, the electronic factors aimed at facilitating the oxidative addition[18] inhibit the reductive elimination process.[4] Effective means

[a] Dr. H. Zhang, X. Luo, H. Duan, Q. Li, L. Zhu, Prof. Dr. A. Lei
College of Chemistry and Molecular Sciences
Wuhan University, 430072 (P. R. China)
Fax: (+86) 27-68754067
E-mail: aiwenlei@whu.edu.cn

[b] K. Wongkhan, Dr. A. S. Batsanov, Prof. Dr. J. A. K. Howard, Prof. Dr. T. B. Marder
Department of Chemistry
Durham University, South Road
Durham DH1 3 LE (UK)
E-mail: todd.marder@durham.ac.uk

[c] Dr. J. Wang
Real-Time Analytics, Mettler Toledo Auto Chem
7075 Samuel Morse Dr., Columbia, MD 21046 (USA)

[d] Prof. Dr. A. Lei
State Key Laboratory of Organometallic Chemistry
Shanghai Institute of Organic Chemistry
Chinese Acadamy of Sciences, 354 Fenglin Lu
Shanghai, 200032 (China)

Supporting information for this article is available on the WWW under http://dx.doi.org/10.1002/chem.200802209.

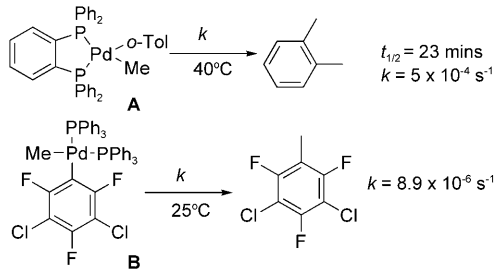

Scheme 1. Selected rate constants for reductive elimination.

to accelerate the reductive elimination are still scarce for cross-coupling reactions involving alkyl groups.

Additives with π-acceptor properties (e.g., maleic anhydride, fumaronitrile, *p*-fluorostyrene, and other olefins) are known to accelerate reductive elimination in stoichiometric reactions.[19–23] They have seldom been used as ligands in catalytic processes.[24–33] Recently, we reported an efficient C_{sp^3}-involved Negishi-coupling catalyzed by a complex of palladium and the phosphine/electron-deficient olefin ligand **1**.[34]

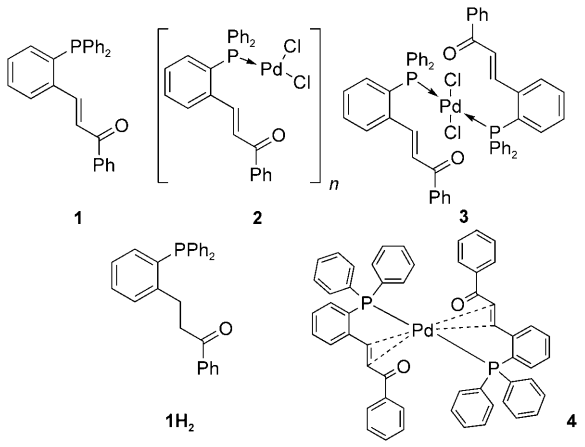

The reaction proceeds exceptionally cleanly, providing a good model for kinetic study. In an attempt to gain a better understanding of the unique role of the ligand, we conducted a series of quantitative kinetic investigations. Herein, we report the finding that ligand **1** dramatically enhances the rate of reductive elimination of a [Ar-Pd-C_{sp^3}] intermediate, thus making alkyl–aryl coupling reactions possible with high efficiency and selectivity, that is, without competing β-hydride elimination.

Results and Discussion

Structures of Pd/phosphine/electron-deficient olefin ligand complexes: Reaction of $[PdCl_2(PhCN)_2]$ with two equivalents of **1** gives **3** in excellent yield (Figure 1, for details see Supporting Information); however, 1:1 reaction gives **2** in solution, which rapidly forms a much less soluble complex

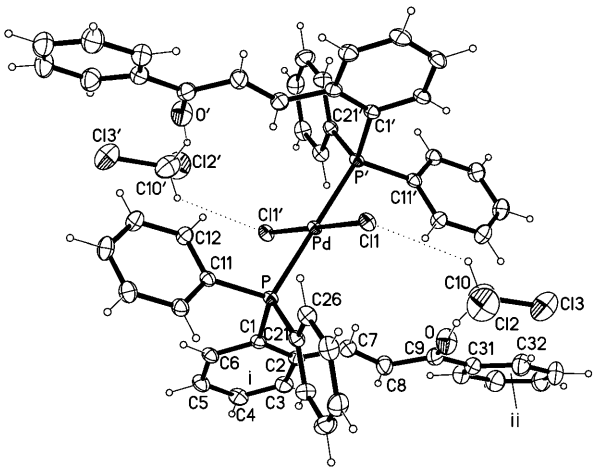

Figure 1. X-ray molecular structure of **3**·2 CH_2Cl_2. The Pd atom lies at an inversion center and has square-planar coordination. Bond lengths (Å): Pd–Cl(1) 2.2973(5), Pd–P 2.3425(6). Thermal ellipsoids are shown at the 50% probability level.

that we formulate as a monophosphine, Cl-bridged dimer or oligomer on the basis of solubility, elemental analysis, solid-state ^{31}P NMR and IR spectroscopy, the last of which shows no sign of alkene bonding to Pd. In contrast, reaction of $[Pd(dba)_2]$ with two equivalents of **1** gives a novel Pd^0 species **4** (Figure 2), in which each of two molecules of **1** are both P- and π-olefin-bound to Pd. Interestingly, in the solid-state structure of **4**, the metal coordination by two P atoms

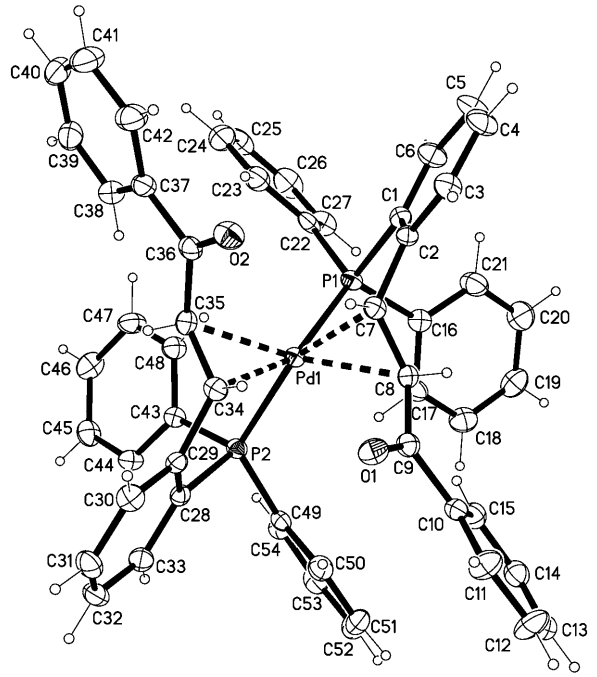

Figure 2. X-ray molecular structure of **4** in **4**·0.5 CH_2Cl_2. Bond lengths in the two independent molecules (Å): Pd–P(1) 2.3776(9) [2.3673(8)], Pd–P(2) 2.3707(8) [2.3545(9)], Pd–C(7) 2.173(3) [2.203(3)], Pd–C(8) 2.289(3) [2.265(3)], Pd–C(34) 2.161(3) [2.144(3)], Pd–C(35) 2.277(3) [2.276(3)].Thermal ellipsoids are shown at the 50% probability level.

and two η^2-olefinic bonds is intermediate between square-planar and tetrahedral, which would be expected for Pd^0 complexes. The plane defined by the Pd atom and the midpoints of both η^2-bonds forms a dihedral angle of 51.8 or 53.1° with the PdP_2 plane (cf. 0 for planar and 90° for tetrahedral coordination). The olefinic C7=C8 bond lengthens from 1.330(3) Å in **3** to the average of 1.406(4) Å in **4** due to metal coordination. The adjacent C2−C7 bond lengthens from 1.467(3) to 1.499(4) Å as the change of the C1-C2-C7-C8 torsion angle from 174.2(3)° in **3** to 57.4(4)–78.1(4)° in **4** breaks the π-conjugation. The angle between aryl planes i and ii increases from 24° in **3** to 67–80° in **4**.[35] For details of the crystal structure and spectroscopic characterization, see Supporting Information.

High-turnover-number (TON) and low-temperature experiments: Figure 3 shows the typical concentration profiles versus time for the reaction [Eq. (1)] of ethyl 2-iodobenzoate (**6**; 100 mmol) with cyclohexylzinc chloride (**7**; 500 mmol) at 25 °C, producing **8** at a final yield of 99 % (determined by GC). The reaction was catalyzed by **2** (0.001 mol %). The turnover frequencies (TOFs) were as high as $10^3\ s^{-1}$. Encouraged by the large TON and TOF values, further kinetic studies were carried out on this Negishi coupling.

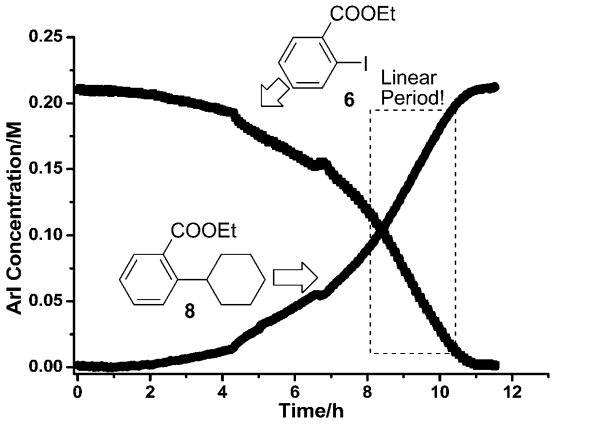

Figure 3. Kinetic profile of reaction of ArI **6** and CyZnCl (**7**) catalyzed by **2** (0.001 mol %) at 25 °C monitored by ReactIR™.

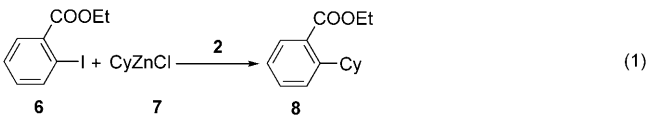

(1)

At 0 °C, with catalyst **2** (0.5 mol %), the coupling of **6** (1.0 mmol) and **7** (2.25 mmol) finished in 17 min (Figure 4A, squares). The same reaction at 15 °C completed within 5 min (Figure 4 A, circles). The high reactivity and selectivity of this reaction demonstrated the capability of the catalyst em-

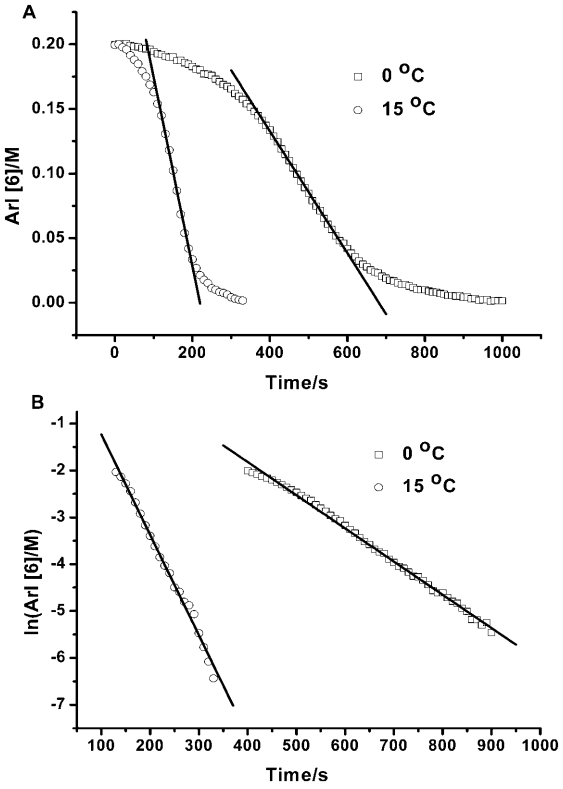

Figure 4. Reaction of ArI **6** and CyZnCl (**7**) catalyzed by **2** (0.001 M) at 0 °C and 15 °C monitored by ReactIR™. A) [**6**] versus time. Linear fit of [**6**] versus time: between 400–600 s (0 °C); between 130–200 s (15 °C). B) Linear fit of ln[**6**] versus time: between 400–900 s (0 °C); between 130–330 s (15 °C).

ployed in enabling the oxidative addition, transmetallation and C_{sp^3}-involved reductive elimination.

The effectiveness of the olefin moiety in ligand 1: The major difference between our catalyst system and the systems reported previously (Scheme 1) was the ligand on the palladium center. Both of the reported cases employed two phosphine ligands, that is, the bidentate chelate, bis(diphenylphosphino)benzene[6] or PPh_3 (2 equiv).[7] Our ligand consists of an electron-deficient olefin in addition to a phosphine moiety.

To elucidate the role of the electron-deficient olefin moiety in the reaction, we examined the coupling of **6** with **9** catalyzed by 1 mol % of complex **3** generated in situ from $[PdCl_2(CH_2CN)_2]$ and ligand **1** (1:2). As expected, and in contrast to catalysis by **2** [Eq. (2)], formation of the desired cross-coupling product **10** was hampered by the presence of the second equivalent of ligand **1**, with only 33 % conversion of **6** after 80 min and a molar ratio of ethyl benzoate to **10** of 1.4:1. In addition, ligand $\mathbf{1}H_2$ was prepared by reduction of the olefin group of ligand **1**, and was utilized in the catalytic coupling of **6** with **9**. The reaction finished after 100 min, but showed poor selectivity, with a molar ratio of ethyl benzoate to **10** of 2:1, indicating that β-hydride elimination is a significant competing process when $\mathbf{1}H_2$ is em-

ployed, again, in contrast to ligand **1**, for which the high selectivity for **10** clearly indicates that reductive elimination must be much faster than β-hydride elimination.

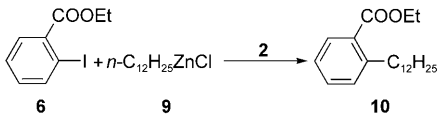

(2)

Catalysis by Pd^0 complexes or Pd nanoparticles (NPs): Literature reports indicate that an inverse order in [Pd] will be observed if a reaction involves the formation of Pd NPs.[36–40] To clarify whether the above reactions were catalyzed by a Pd^0 complex or Pd NPs, we carried out kinetic experiments using different Pd loadings (from 0.25 mol% to 2 mol%), with all other factors held constant. The results are shown on Figure 5. Clearly, we can see that the reaction is first-order in [Pd]. In addition, the intercept is almost zero, which strongly indicates that the reaction is taking place mainly through a single pathway. This is consistent with homogeneous catalysis by Pd complexes rather than by Pd NPs. Ligand inhibition experiments are another way to identify catalytic processes involving NPs, in which less than one equivalent of ligand (vs. catalyst) can completely shut down the reactivity. Thus, we examined the reaction in the presence of catalyst **2** (1 mol%) and PPh_3 (0.3 mol%), and found that the reaction was somewhat slower (Figure 6). In comparison, when $Pd(OAc)_2$ (1 mol%) was used as the catalyst precursor, the reaction of ArI **6** and alkylzinc **9**, which normally is complete within scores of seconds, was extremely slow when 0.3 mol% PPh_3 was added (Figure 6). Again, this supports our proposal that catalyst **2** is homogeneous, whereas $Pd(OAc)_2$ generates Pd NPs.[41,42]

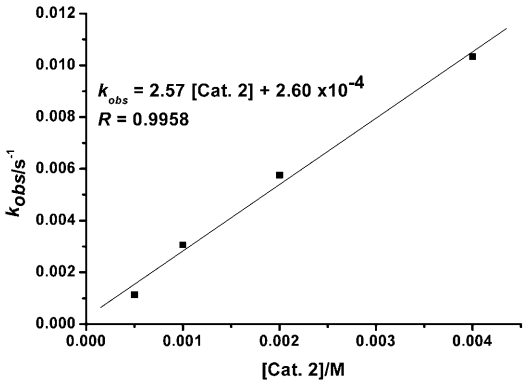

Figure 5. The k_{obs} of reactions between ArI **6** and $R_{alkyl}ZnCl$ **9** catalyzed by **2** (0.0005, 0.001, 0.002, 0.004 M) at 15 °C monitored by ReactIR™.

The rates of reductive elimination determined from the zero-order kinetic regime: Figures 3 and 4A both revealed an induction period, during which the rate accelerated until transitioning into a zero-order kinetic regime. Such an induction period may be explained by slow generation of the active catalytic species. The plot of concentration versus time for the 0 °C experiment (Figure 4A) indicates clearly that the rate continued to increase sharply until about 33% conversion, then the rate was almost unchanged until about 79% conversion. The same trend was found for the 15 °C experiment.

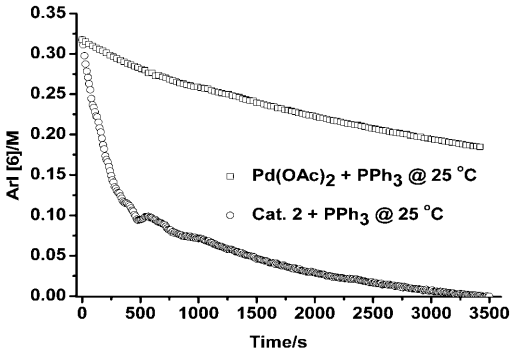

Figure 6. Reactions of ArI **6** with $R_{alkyl}ZnCl$ **9** catalyzed by **2** or $Pd(OAc)_2$ at 25 °C monitored by ReactIR™. For both experiments before ArI **6** was added to initiate reaction, 0.3 equiv PPh_3 (vs. **2** or $Pd(OAc)_2$) was added and mixing for 5 min.

Due to the long induction period of the reaction between **6** and **7**, the global kinetics was difficult to study. The reaction of **6** with **9** was investigated [Eq. (2)]. Because of the conformational restriction of a cyclohexyl group, the reduction of Pd^{II} to Pd^0 by **7** might be a slower process compared to that by alkylzinc **9**. The reaction progress was monitored in situ by ReactIR™. Pleasantly, the induction period disappeared as expected (Figure 7A). This result further supported the hypothesis that the observed induction period was due to the slow formation of an active catalyst, through interaction between **2** and the alkylzinc reagent.

A distinct kinetic feature of this catalytic reaction is the existence of a zero-order kinetic regime, with or without the induction period (e.g., Figure 4A (after the induction period) and Figure 7A). As shown in Scheme 2, the Negishi reaction follows a general pathway involving sequential oxidative addition (k_{OA}), transmetallation (k_{TM}), and reductive elimination (k_{RE}). Within the zero-order kinetic regime, the reaction rate is independent of the concentrations of both starting materials (i.e., ArI and RZnX). The fact that the rate appears to be zero-order in both [ArI] and [RZnX] between certain conversions, indicates that neither the oxidative addition nor the transmetallation was the rate-determining step. Therefore, within this zero-order kinetic regime, the reaction rate could be limited by the reductive elimination step (k_{RE}).[43,44] The rate constants for reductive elimination k_{RE} were then obtained from fitting the experimental data, and the results are listed in Tables 1 and 2. The rate constants for reductive elimination in the reaction of **6** with **7** were 0.472, and 1.46 s^{-1} at 0 °C and 15 °C, respectively. The rate constant for reductive elimination in the reaction **6** with **9** was about 0.3 s^{-1} at 15 °C (Table 2). These rate constants

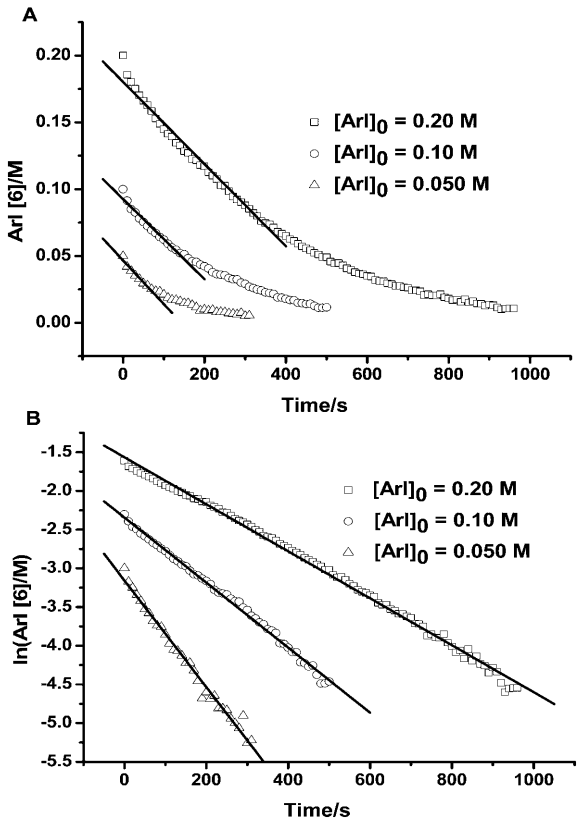

Figure 7. Reaction of ArI **6** with $R_{alkyl}ZnCl$ **9** catalyzed by **2** (0.001 M) at 15 °C monitored by ReactIR™. A) Kinetic profile of **6** versus time, treated as a zero order reaction, that is, reductive elimination is the rate-determining step. B) Treated as a first-order reaction, that is, oxidative addition is the rate-determining step.

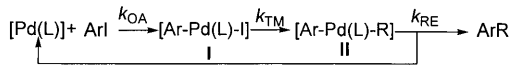

Scheme 2. The proposed catalytic cycle.

Table 1. Rate constants of reaction [Eq. (1)] involving CyZnCl.

	T [°C]	Conversion [%]	k_{obs}[a]	k_{OA} [$M^{-1}s^{-1}$]	k_{RE} [s^{-1}]
zero	0	33–79	4.72×10^{-4}	N.A.	0.472
order	15	35–83	1.46×10^{-3}	N.A.	1.46
first	0	33–98	7.08×10^{-3}	7.08	$\gg1.4$[b]
order	15	35–99	2.14×10^{-2}	21.4	$\gg4.3$[b]

[a] The unit of k_{obs} for the zero order reaction is s^{-1}, the unit of k_{obs} for the first-order reaction is Ms^{-1}. [b] Under these conditions, oxidative addition is deemed to be the rate-determining step, the rate of reductive elimination is much faster than oxidative addition, so k_{RE} is expressed as $\gg k_{OA}\times[ArI]_0$.

are far greater than those reported by both Hartwig ($5\times10^{-4}\,s^{-1}$)[6] and Espinet ($8.9\times10^{-6}\,s^{-1}$),[7] which might reveal the effects of designed ligand **1** on the reductive elimination step by comparison with dppbz and $(PPh_3)_2$.[45]

The rates of reductive elimination determined from the first-order kinetic regime: As Figure 4 showed, ln[**6**] plotted versus time, gave a better linear fit in the range of conversion of 33–98% for the experimental data of the reaction of **6** with CyZnCl **7** (Figure 4B, and Table 1). Similar kinetic analysis was obtained for the reaction of **6** with alkylzinc **9** (Figure 7B and Table 2). In this regard, first-order kinetics was assigned to the decline of ArI **6**, which meant that oxidative addition was the rate-determining step, and the rate constants for reductive elimination should be $\gg[\mathbf{6}]\times k_{OA}$. By linear fitting of ln[**6**] versus time (Figures 4B and 7B), two sets of k_{RE} were obtained, listed in Tables 1 and 2. Although the exact value of k_{RE} cannot be obtained, they are certainly much larger than the reported numbers shown in Scheme 1.

Table 2. Rate constants for the reaction [Eq. (2)] involving n-$C_{12}H_{25}ZnCl$ at 15 °C.

	$[ArI]_0$ [M]	Conversion	k_{obs}[a]	k_{OA} [$M^{-1}s^{-1}$]	k_{RE} [s^{-1}]
zero	0.20	0–67%	3.07×10^{-4}	N. A.	0.307
order	0.10	0–49%	2.99×10^{-4}	N. A.	0.299
	0.050	0–50%	3.27×10^{-4}	N. A.	0.327
first	0.20	0–95%	3.03×10^{-3}	3.03	$\gg0.6$[b]
order	0.10	0–88%	4.20×10^{-3}	4.20	$\gg0.4$[b]
	0.050	0–89%	6.88×10^{-3}	6.88	$\gg0.7$[b]

[a] The unit of k_{obs} for the zero order reaction is s^{-1}, the unit of k_{obs} for the first-order reaction is Ms^{-1}. [b] Under these conditions, OA is deemed to be the rate-determining step; the rate of RE is much faster than OA, so k_{RE} is expressed as $\gg k_{OA}\times[ArI]_0$.

The rates of reductive elimination determined from the more complex kinetic regime: Although each single experiment gave a good first-order fit, surprisingly, the k_{obs} from three runs of the reaction of **6** with **9** using three different $[\mathbf{6}]_0$, which should be same, are different (Table 2). The kinetic data might indicate that the reaction is more complex. If we consider that reductive elimination is not rate-limiting, and with the steady state approximation, the rate equation can be expressed as Equation (3) (see the Supporting Information for detailed mathematical deduction), in which one can see that there is no simple order for electrophile **6** or nucleophile **9**.

$$\text{rate} = \frac{k_1k_2[ArI][RZnCl][Pd]_{total}}{k_1[ArI]+k_2[RZnCl]} \quad (3)$$

To see whether catalyst deactivation was involved or not in this reaction, according to Blackmond's theory of "reaction progress kinetic analysis",[43,44] the "same excess" experiments (see Supporting Information for detailed explanation) were investigated. Figure 8 shows the results of these "same excess" experiments, clearly indicating some degree of catalyst deactivation.

Based on the proposed catalytic pathway in Scheme 2, assuming that reductive elimination is not the rate-determining step, and that there is catalyst deactivation (we regarded this deactivation as a first-order process, with rate constant, k_{decay}),[46] kinetic simulation was used to obtain the rate constant.[47,48] The fitting of the reaction mechanism to the experimental curves was performed with the kinetic simulator software Dynafit.[48] The results are listed in Figure 9 and Table 3. The rate constant for oxidative addition (k_{OA}) is

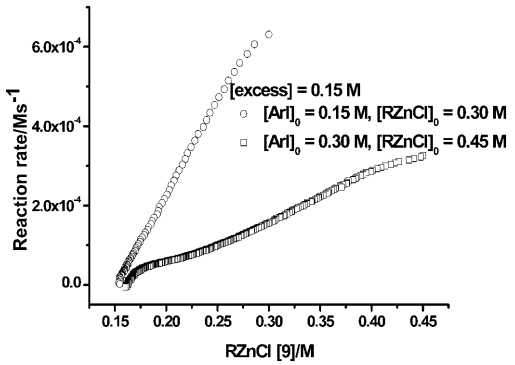

Figure 8. The "same excess" experiments for reaction between ArI **6** and $R_{alkyl}ZnCl$ **9** catalyzed by **2** (0.001 M) at 15 °C.

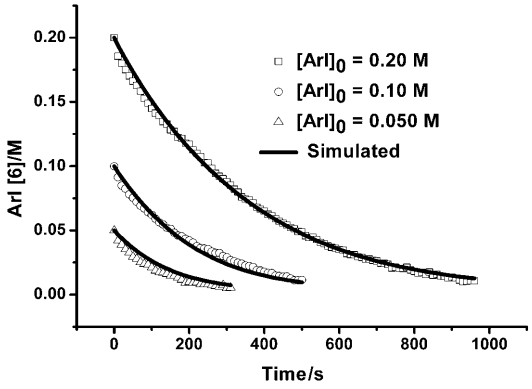

Figure 9. The simulated curve and the experimental data of reaction between ArI **6** and $R_{alkyl}ZnCl$ **9** catalyzed by **2** (0.001 M) at 15 °C.

Table 3. Rate constants determined by fitting the experimental data of Figure 7A with Dynafit.

	k_{OA} [$M^{-1}s^{-1}$]	k_{TM} [$M^{-1}s^{-1}$]	K_{decay} [s^{-1}]	k_{RE} [s^{-1}]
constant	10.8	2.50	2.55×10^{-3}	$\geqslant 0.5$[a]
error	0.51	0.57	2.1×10^{-4}	

[a] Under these conditions, the rate of reductive elimination is deemed to be much faster than oxidative addition or transmetallation, so k_{RE} is expressed as $\geqslant k_{OA}\times[ArI]_0$ or $k_{TM}\times[RZnCl]_0$.

10.8 M s^{-1} and k_{TM} is 2.5 M s^{-1}. The exact value of rate constant for reductive elimination was not obtained from this kinetic analysis, while it can be expressed as $k_{RE}\geqslant k_{OA}\times[ArI]_0$ or $k_{RE}\geqslant k_{TM}\times[RZnCl]_0$. It is $k_{RE}\geqslant 0.5\ s^{-1}$, which of course, is far greater than the reported values in Scheme 1.[6,7]

In other words, no matter how we treated the experimental data as zero-order (the rate-determining step was reductive elimination) or first-order, or even with a more complicated kinetic profile in which reductive elimination is not rate-determining, in the two last cases, the rate constants for reductive elimination are about four orders of magnitude greater than that reported by Hartwig[6] and about five orders of magnitude greater than that reported by Espinet.[7]

Conclusion

The results from the experiments above manifested the effects of the olefin part of ligand **1** in enhancing the C_{sp^2}–C_{sp^3} cross-coupling reaction, particularly in terms of the reductive elimination rate. It is reasonable to conclude that the olefin moiety in **1**, with good π-acceptor properties, accelerated the reductive elimination of an [Ar-Pd-C_{sp^3}] species, thus resulting in the highly selective and efficient coupling reaction. These results provide new insight into ligand design for C–C coupling reactions. For example, **1** is a highly effective ligand for Pd-catalyzed C_{sp}–C_{sp} cross-coupling reactions.[49] Further applications of ligand **1** are under active investigation in our laboratories.

Experimental Section

Typical procedure for ReactIR™ experiments: Compound **2** (0.001 mmol) and CyZnCl (**7**; 1 M, 500 mL) were placed in a 3-necked vessel, and then ethyl 2-iodobenzoate (**6**; 28 g, 0.1 mol) was added to initiate the reaction. The mixture was monitored by ReactIR™ at 25 °C. During the reaction, aliquots were removed and analyzed by GC, and the results were used to calibrate the ReactIR™ spectra and to obtain the conversion and yield. At the end of the reaction, no ArI **6** was detected, and a 99% GC yield was obtained for the cross-coupling product **8**.

Acknowledgement

This work was support by National Natural Science Foundation of China (20502020, 20702040, 20832003) and a startup fund from Wuhan University. K.W. thanks the Royal Thai Government for a postgraduate scholarship. Q.L. thanks the China Scholarship Council for a Fellowship to work at Durham University. T.B.M. thanks the Royal Society of Chemistry for a Journals Grant for International Authors and Durham University for an HEIF Grant.

[1] F. Diederich, P. J. Stang, *Metal-Catalyzed Cross-Coupling Reactions*, 2nd ed., Wiley-VCH, Weinheim, **2004**.
[2] E.-i. Negishi, *Handbook of Organopalladium Chemistry for Organic Synthesis*, Wiley, New York, **2002**.
[3] D. J. Cárdenas, *Angew. Chem.* **1999**, *111*, 3201–3203; *Angew. Chem. Int. Ed.* **1999**, *38*, 3018–3020.
[4] D. J. Cárdenas, *Angew. Chem.* **2003**, *115*, 398–401; *Angew. Chem. Int. Ed.* **2003**, *42*, 384–387.
[5] T.-Y. Luh, M.-k. Leung, K.-T. Wong, *Chem. Rev.* **2000**, *100*, 3187–3204.
[6] D. A. Culkin, J. F. Hartwig, *Organometallics* **2004**, *23*, 3398–3416.
[7] J. A. Casares, P. Espinet, B. Fuentes, G. Salas, *J. Am. Chem. Soc.* **2007**, *129*, 3508–3509.
[8] N. Kataoka, Q. Shelby, J. P. Stambuli, J. F. Hartwig, *J. Org. Chem.* **2002**, *67*, 5553–5566.
[9] D. W. Old, J. P. Wolfe, S. L. Buchwald, *J. Am. Chem. Soc.* **1998**, *120*, 9722–9723.
[10] G. Altenhoff, R. Goddard, C. W. Lehmann, F. Glorius, *Angew. Chem.* **2003**, *115*, 3818–3821; *Angew. Chem. Int. Ed.* **2003**, *42*, 3690–3693.
[11] O. Navarro, R. A. Kelly III, S. P. Nolan, *J. Am. Chem. Soc.* **2003**, *125*, 16194–16195.
[12] M. Eckhardt, G. C. Fu, *J. Am. Chem. Soc.* **2003**, *125*, 13642–13643.
[13] J. E. Milne, S. L. Buchwald, *J. Am. Chem. Soc.* **2004**, *126*, 13028–13032.

[14] B. C. Hamann, J. F. Hartwig, *J. Am. Chem. Soc.* **1998**, *120*, 7369–7370.
[15] A. F. Littke, G. C. Fu, *J. Org. Chem.* **1999**, *64*, 10–11.
[16] C. Dai, G. C. Fu, *J. Am. Chem. Soc.* **2001**, *123*, 2719–2724.
[17] N. Hadei, E. A. B. Kantchev, C. J. O'Brien, M. G. Organ, *Org. Lett.* **2005**, *7*, 3805–3807.
[18] A. F. Littke, G. C. Fu, *Angew. Chem.* **2002**, *114*, 4350–4386; *Angew. Chem. Int. Ed.* **2002**, *41*, 4176–4211.
[19] A. Yamamoto, S. Ikeda, *J. Am. Chem. Soc.* **1967**, *89*, 5989–5990.
[20] T. Yamamoto, A. Yamamoto, S. Ikeda, *J. Am. Chem. Soc.* **1971**, *93*, 3350–3359.
[21] R. Sustmann, J. Lau, *Chem. Ber.* **1986**, *119*, 2531–2541.
[22] A. E. Jensen, P. Knochel, *J. Org. Chem.* **2002**, *67*, 79–85.
[23] T. Yamamoto, M. Abla, Y. Murakami, *Bull. Chem. Soc. Jpn.* **2002**, *75*, 1997–2009.
[24] R. Giovannini, T. Studemann, G. Dussin, P. Knochel, *Angew. Chem.* **1998**, *110*, 2512–2515; *Angew. Chem. Int. Ed.* **1998**, *37*, 2387–2390.
[25] R. Giovannini, T. Stuedemann, A. Devasagayaraj, G. Dussin, P. Knochel, *J. Org. Chem.* **1999**, *64*, 3544–3553.
[26] M. A. Grundl, J. J. Kennedy-Smith, D. Trauner, *Organometallics* **2005**, *24*, 2831–2833.
[27] A. Scrivanti, V. Beghetto, U. Matteoli, S. Antonaroli, A. Marini, B. Crociani, *Tetrahedron* **2005**, *61*, 9752–9758.
[28] D. B. G. Williams, M. L. Shaw, *Tetrahedron* **2007**, *63*, 1624–1629.
[29] I. J. S. Fairlamb, A. R. Kapdi, A. F. Lee, G. P. McGlacken, F. Weissburger, A. H. M. de Vries, L. Schmieder-van de Vondervoort, *Chem. Eur. J.* **2006**, *12*, 8750–8761.
[30] I. J. S. Fairlamb, A. R. Kapdi, A. F. Lee, *Org. Lett.* **2004**, *6*, 4435–4438.
[31] Y. Mace, A. R. Kapdi, I. J. S. Fairlamb, A. Jutand, *Organometallics* **2006**, *25*, 1795–1800.
[32] I. J. S. Fairlamb, *Org. Biomol. Chem.* **2008**, *6*, 3645–3656.
[33] P. S. Pregosin, *Chem. Commun.* **2008**, 4875–4884.
[34] X. Luo, H. Zhang, H. Duan, Q. Liu, L. Zhu, T. Zhang, A. Lei, *Org. Lett.* **2007**, *9*, 4571–4574.
[35] CCDC 701728 (**3**) and 701729 (**4**) contain the supplementary crystallographic data for this paper. These data can be obtained free of charge from The Cambridge Crystallographic Data Centre via www.ccdc.cam.ac.uk/data_request/cif; Crystal data for **3**: $C_{54}H_{42}Cl_2O_2P_2Pd{\cdot}2\,CH_2Cl_2$, $M_r=1131.97$, $T=120$ K, monoclinic, space group $P2_1/n$, $a=9.0882(8)$, $b=25.761(2)$, $c=11.379(1)$ Å, $\beta=106.49(1)°$, $V=2554.4(4)$ Å^3, $Z=2$, $\rho_{calcd}=1.472$ g cm^{-3}, $\mu=0.78$ mm^{-1}, 34743 reflections with $2\theta=60°$, 7423 unique, $R_{int}=0.033$, $R(F)=0.040$ [6286 data with $I=2\sigma(I)$], w$R(F^2)=0.113$ (all data). Crystal data for **4**: $C_{54}H_{42}O_2P_2Pd{\cdot}0.5\,CH_2Cl_2$, $M_r=933.68$, orthorhombic, space group $Pca2_1$, $a=38.814(6)$, $b=10.691(2)$, $c=20.880(3)$ Å, $V=8664(2)$ Å^3; $Z=8$, $\rho_{calcd}=1.432$ g cm^{-3}, $\mu=0.61$ mm^{-1}, 73864 reflections with $2\theta=56°$, 17706 unique, $R_{int}=0.047$, $R(F)=0.031$ [15582 data with $I=2\sigma(I)$], w$R(F^2)=0.065$ (all data).
[36] M. T. Reetz, J. G. de Vries, *Chem. Commun.* **2004**, 1559–1563.
[37] I. J. S. Fairlamb, S. Grant, P. McCormack, J. Whittall, *Dalton Trans.* **2007**, 859–865.
[38] G. P. F. Van Strijdonck, M. D. K. Boele, P. C. J. Kamer, J. G. de Vries, P. W. N. M. Van Leeuwen, *Eur. J. Inorg. Chem.* **1999**, 1073–1076.
[39] I. J. S. Fairlamb, R. J. K. Taylor, J. L. Serrano, G. Sanchez, *New J. Chem.* **2006**, *30*, 1695–1704.
[40] A. H. M. de Vries, J. M. C. A. Mulders, J. H. M. Mommers, H. J. W. Henderickx, J. G. de Vries, *Org. Lett.* **2003**, *5*, 3285–3288.
[41] While Pd NPs are also known to be effective catalysts for this transformation,[42] both the clear first-order dependence on [Pd] and the results of PPh_3 inhibition experiments (see text and Supporting Information for details) ruled them out as being active species in the present case.
[42] J. Liu, Y. Deng, H. Wang, H. Zhang, G. Yu, H. Zhang, Q. Li, T. B. Marder, Z. Yang, A. Lei, *Org. Lett.* **2008**, *10*, 2661–2664.
[43] J. S. Mathew, M. Klussmann, H. Iwamura, F. Valera, A. Futran, E. A. C. Emanuelsson, D. G. Blackmond, *J. Org. Chem.* **2006**, *71*, 4711–4722.
[44] D. G. Blackmond, *Angew. Chem.* **2005**, *117*, 4374–4393; *Angew. Chem. Int. Ed.* **2005**, *44*, 4302–4320.
[45] Hartwig reported reductive elimination involving an electronic-rich aryl group, and Espinet employed an electron-poor aryl group. Although the substrates in our system, which involved an electron-poor aryl group, were different from theirs, the data still indicate the dramatic accelerating effect on reductive elimination.
[46] G. Rothenberg, S. C. Cruz, G. P. F. Van Strijdonck, H. C. J. Hoefsloot, *Adv. Synth. Catal.* **2004**, *346*, 467–473.
[47] C. S. Consorti, F. R. Flores, J. Dupont, *J. Am. Chem. Soc.* **2005**, *127*, 12054–12065.
[48] P. Kuzmic, *Anal. Biochem.* **1996**, *237*, 260–273.
[49] W. Shi, Y. Luo, X. Luo, L. Chao, H. Zhang, J. Wang, A. Lei, *J. Am. Chem. Soc.* **2008**, *130*, 14713–14720.

Received: October 25, 2008
Published online: February 19, 2009

